The role of XAFS in the *in situ* and *ex situ* elucidation of active sites in designed solid catalysts

John Meurig Thomas* and Gopinathan Sankar

Davy Faraday Research Laboratory, The Royal Institution of GB, 21 Albemarle Street, London W1S 4BS, England.
E-mail: jmt@ri.ac.uk

New mesoporous and microporous catalysts based on silica, aluminophosphates, or aluminophosphates containing one or other of the heteroatoms Ti, Co, Mn, Fe and Cr, are ideally suited for study by X-ray absorption fine structure (XAFS). The information derived from X-ray absorption near-edge structure (XANES) and extended X-ray absorption fine structure (EXAFS) elucidates the nature of the catalytically active site, generally (but not invariably) under *in situ* conditions. This, in turn, provides new insights into the mechanism of the catalysis and suggests methods of improving the performance of the original catalyst. In this way, significant advances have recently been made in designing catalysts for the selective oxidation of alkanes, for the epoxidation of alkenes and for the dehydration of alcohols to yield olefins. Combined with density functional theory (DFT) computations, XAFS studies have also yielded fresh insights into the architecture of nanoparticle catalysts, such as $Ru_{12}Cu_4C_2$ supported on mesoporous silica.

Keywords: catalysts; mesoporous; microporous; silica; aluminophosphates.

1. Introduction

We are concerned here with high-area microporous or mesoporous solids consisting of silica, aluminophosphates or aluminosilicates in which the locus of catalytic conversion, the so-called active site, has been introduced (grafted) either after formation of the high-area solid or during the course of its synthesis. Such open-structure high-area solids facilitate access (*i.e.* diffusion) of reactants to, and products away from, the active sites that are situated at their internal surfaces. They are typical of the kind of catalysts used extensively in industry. This is one reason why they constitute admirable targets for structural elucidation: such fundamental information as is retrieved is not only of academic interest, it is immediately relevant to commercially important situations (Thomas & Thomas, 1997; Ertl *et al.*, 1997).

But microporous and mesoporous catalysts possess a second advantage in that they are readily amenable to *in situ* study by a wide range of investigative tools, covering essentially all the spectroscopic techniques as well as X-ray and neutron diffraction (Thomas, 1997). Moreover, they are particularly convenient targets for study by synchrotron-based techniques such as X-ray absorption spectroscopy (XAS), X-ray diffraction (XRD) (separately or in combination) (Couves *et al.*, 1991; Thomas & Greaves, 1994; Clausen & Topsøe, 1996; Als-Nielsen *et al.*, 1995; Thomas *et al.*, 1995; Sankar *et al.*, 1993, 2000; Clausen *et al.*, 1998; Sankar & Thomas, 1999), and, if required, by the additional use of small-angle X-ray scattering (SAXS) (Aletru *et al.*, 1999). Using experimental setups such as those schematized in Fig. 1, both *in situ* studies (involving gas–solid systems and atmospheric pressure or higher, and at temperatures well beyond 873 K, or liquid–solid systems up to *ca* 423 K) and *ex situ* studies, such as those highlighted below, may be readily conducted.

2. Summarized aims

One of the reasons why such dramatic advances have been made in the study of the mode of action of metallo-enzymes is because detailed structural information pertaining to the metal-centred active sites has been retrieved through the application of high-resolution X-ray diffraction to these enzymes under operating conditions. For the inorganic open-structure oxides (both as such or with heteroatoms grafted on to them), the initial aim is to deploy XAFS either alone (the concentration of heteroatoms is invariably restricted to below 10 wt%) or, preferably, in combination with other techniques (usually XRD or computational approaches). The ultimate aim, however, is to be in a position, after acquiring a precise knowledge of the atomic environment of a catalytically active site, to prepare catalysts of superior performance by modifying both the composition and structure of the active site.

There are five distinct categories of catalyst, which we will focus upon here: (i) titanium-centred epoxidation catalysts (§3.1); (ii) chromium–silica catalyst for the polymerization of ethylene (§3.2); (iii) bimetallic, nanoparticle catalysts (*e.g.* CuRu or PdRu catalysts) supported on silica for the selective hydrogenation of unsaturated hydrocarbons (§3.3); (iv) and (v), molecular sieve catalysts for the aerial (selective) oxidation of alkanes and iron-centred microporous catalysts for the shape-selective conversion of cyclohexane to adipic acid in air (§3.4). Full experimental details of how these various kinds of catalysts are investigated *in situ* or *ex situ* will emerge during the course of discussions of each.

3. The catalysts

3.1. *Epoxidation catalysts based on titanium*

For some 20 years, the conversion of propylene to propylene oxide,

$$CH_3-CH=CH_2 \longrightarrow CH_3-\underset{\displaystyle O}{\overset{/\quad\backslash}{CH-CH_2}} \qquad (1)$$

has been effected by a so-called Ti/SiO_2 catalyst (developed by Shell Co.) which, in the presence of alkylhydroperoxides, typified by tertiary butyl hydroperoxide (TBHP), smoothly converts the propylene to the epoxide, which is an important building block in the chemical industry (Murugavel & Roesky, 1997).

Until very recently, the nature of the active site at which the propylene (or any other alkene) is converted to the epoxide was the subject of much uncertainty and speculation (see Fig. 2*a*).

Using a well defined procedure (Maschmeyer *et al.*, 1995) for the preparation of single isolated titanium-centred active sites on a mesoporous silica (labelled MCM-41) from a titanocene dichloride precursor, it was established by XAFS (extended edge and near edge) (see Fig. 2*b*) that the active site is a Ti^{IV} ion tripodally attached to the underlying silica *via* three $-O-Si$ bonds and containing one titanol bond ($Ti-OH$) which stands proud of the surface. There is no evidence from XAFS whatsoever for the occurrence of any titanyl groups (top part of Fig. 2*a*) and, at most, only traces of the bipodally attached di-titanol structure are found (bottom part of Fig. 2*a*). We can also rule out, on the basis of our independent work (Roberts *et al.*, 1996) on minerals (such as fresnoite) and their synthetic analogues (such as JDF-L1), which by XAFS and XRD are shown to contain short $Ti{=}O$ groups and a five-coordinated central Ti^{IV} ion,

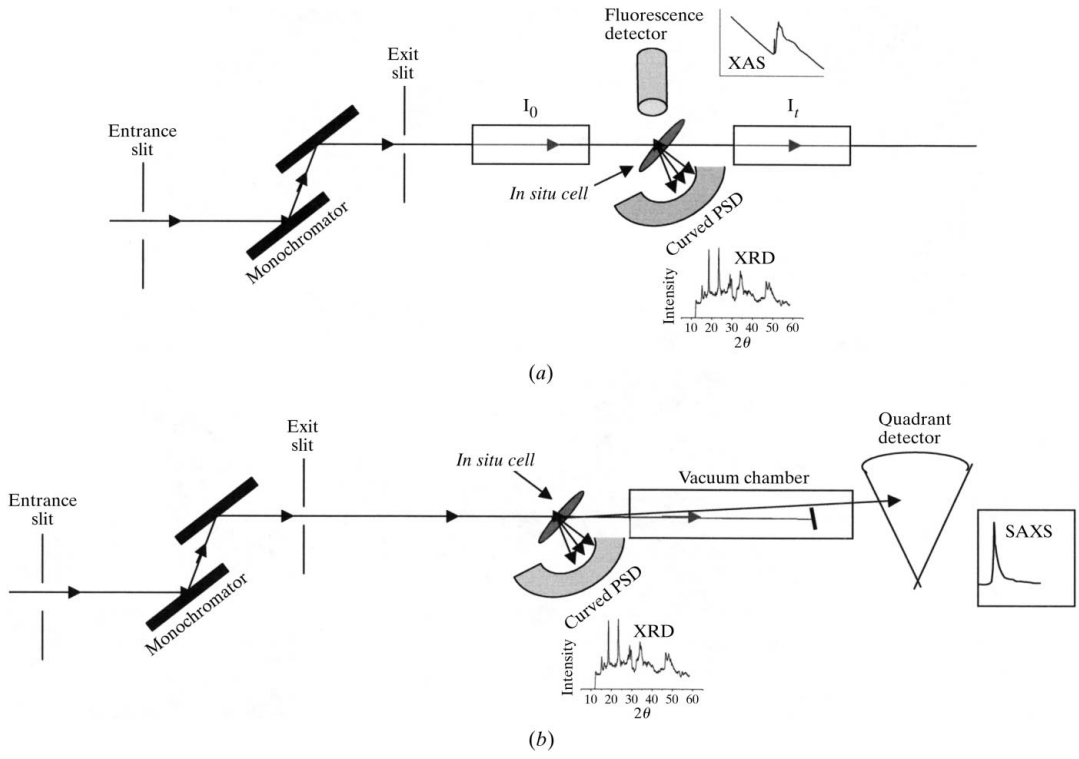

Figure 1
Schematic diagram of the experimental setup used for combined (*a*) EXAFS/XRD and (*b*) SAXS/WAXS experiments. I_o and I_t are the ionization chambers used to measure the incident and transmitted beam, respectively. The fluorescence detector used at station 9.3 is a 13-element Canberra detector.

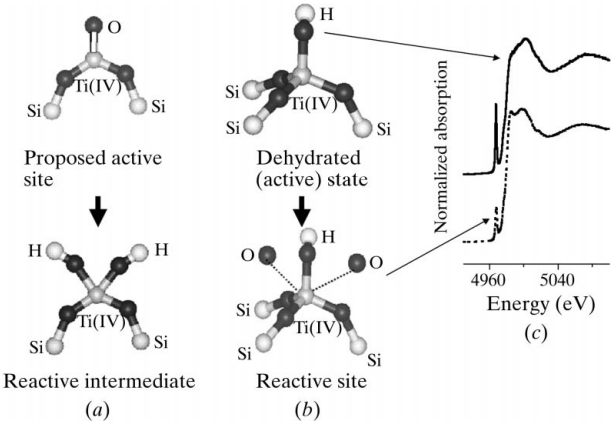

Figure 2
Schematic representation of (*a*) the proposed structure for the active titanium centres (see Sheldon, 1983) and (*b*) the local structure of the titanium centres in the dehydrated and reactive state determined by EXAFS. (*c*) The corresponding Ti *K*-edge XANES spectra of the Ti↑MCM-41 catalyst.

that there is any five-coordination in the as-prepared Ti^{IV}-centred active site in its non-reacted state. By conducting *in situ* XANES and EXAFS studies of the active Ti↑MCM-41 (Fig. 3) epoxidation catalyst, one may obtain direct evidence for the expansion of the coordination shell (from fourfold) to close to distorted sixfold coordination during the course of catalytic turnover (Figs. 2*b* and 2*c*).

It has also been possible to boost the catalytic activity of the titanium-centred silica catalyst by preparing samples in which one of the three silicons to which the Ti^{IV} is tripodally attached is replaced by a germanium atom (Oldroyd *et al.*, 1997). Moreover, using soluble titanosilsesquioxanes, and also modifying the immediate environment of the titanium atoms, it can be shown that there is a near-identity between the active site in the heterogeneous and homogeneous epoxidation catalysts (Thomas *et al.*, 1999*a*).

3.2. *Chromium silica polymerization catalysts*

The discovery by the Philips Company many years ago that traces of chromium inserted into a high-area silica support (such as silica gel) functions as a powerful catalyst for the production of polyethene from ethene, has led to intense debate regarding the cause of the catalytic activity. Over the past 20 years, every single oxidation state of chromium, from II to VI, has been cited as the root cause.

Guided by data acquired for a range of model chromium-containing compounds with various kinds of Cr–O coordination (Fig. 4*a*), we undertook (Nishimura *et al.*, 2001; Nishimura, 1993) *in situ* XAS studies of silica supports on to which chromium was grafted *via* gaseous chromyl chloride CrO_2Cl_2. It is clear that in the calcined (non-catalytically active) state, Cr^{VI} ions in fourfold coordination are dominant. By exposure of this sample to carbon monoxide at *ca* 673 K, a procedure well known to convert the material into a catalytically active state, we find that the Cr^{II} oxidation state predominates (Fig. 4*b*).

In the as-synthesized state of CrAlPO-5 (chromium-substituted aluminophosphate number 5), XAFS analysis (*ex situ*) shows that there are Cr^{III} ions in octahedral environments. But in the calcined state, where the solid acts as a good catalyst for the selective decomposition of cyclohexyl hydroperoxide into cyclohexanone, it is found that some 40% of the chromium is now in the Cr^{VI} state and in tetrahedral coordination (Fig. 5).

When chromium ions are incorporated into the framework structure of mesoporous silica (such as MCM-41), both XAFS and FTIR (Fourier transform infrared) spectra reveal the existence of a certain fraction of Cr═O groups (Rey *et al.*, 1996), just as there are V═O

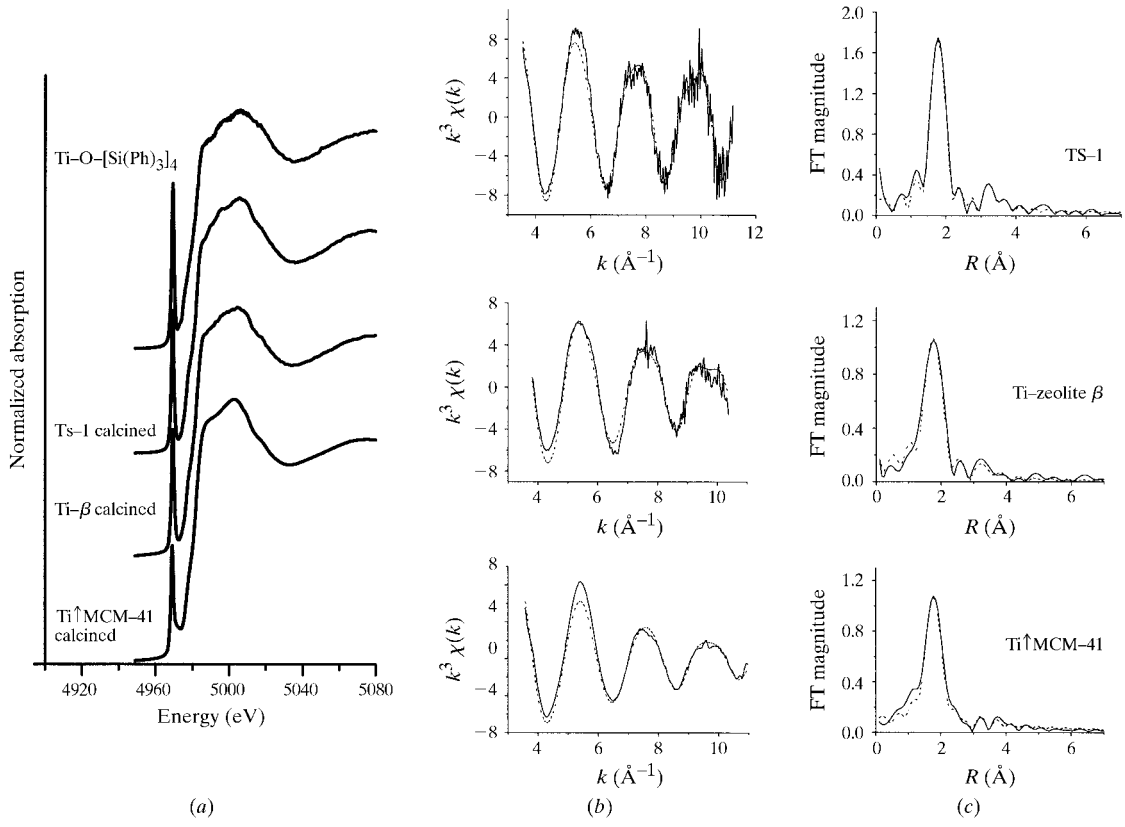

Figure 3
Ti *K*-edge (*a*) XANES and (*b*) EXAFS, along with (*c*) the associated Fourier transforms of titanium-containing micro- and mesoporous catalysts employed for the epoxidation of alkenes. The solid lines in (*b*) and (*c*) represents the experimental data and the dashed curves show the EXAFS calculated using the program *EXCURV*98. The details of the curve-fitting analysis have been presented by Gleeson *et al.* (2000).

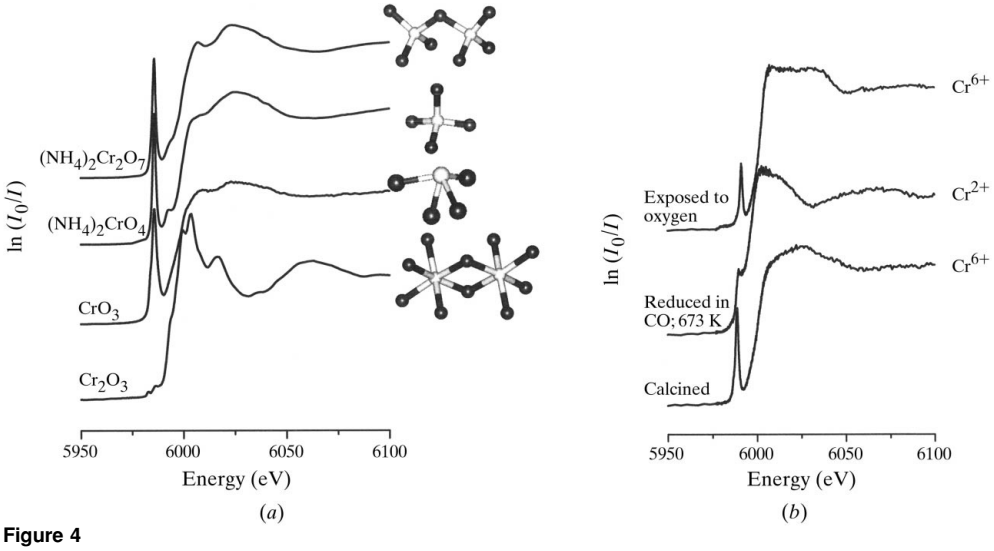

Figure 4
(*a*) Cr *K*-edge XANES of a few model compounds in which chromium ions are present in either the VI or III oxidation state. (*b*) XANES spectra of the calcined (at 873 K in oxygen) Cr(0.5 wt%)/SiO_2 catalyst, of the catalyst reduced in CO at 673 K, and of the catalyst exposed to atmospheric oxygen after reduction.

groups in surface layers of vanadia–titania (Kozlowski *et al.*, 1983) and vanadium-containing MCM-41 (Oldroyd *et al.*, 1998) catalysts.

3.3. *Bimetallic nanoparticle catalysts*

When the physical dimension of a catalyst particle is less than *ca* 50 Å diameter, XRD is of little value as a structural probe since the active material is essentially X-ray amorphous. XAS, however, is better equipped (but not totally satisfactorily; see below) to investigate such materials, as is seen in studies of CuRu (Shephard *et al.*, 1998; Thomas, 1999) and RuPd (Thomas, 1999; Raja *et al.*, 1999) nanocrystals of some 15 Å diameter.

Such well defined bimetallic nanocrystals are conveniently prepared by first anchoring and then gently thermolysing the bimetallic (mixed metal) anions, such as $[Ru_6C(CO)_{16}.Cu_2Cl]^{2-}$ and $[Ru_6Pd_6(CO)_{24}]^{2-}$ on to the inner walls of mesoporous silica specimens such as MCM-41. FTIR spectroscopy serves as a good indicator of when the organic drapery attached to the bimetallic cone has been driven off. All the while, detailed *in situ* measurements of the XANES and EXAFS features of these materials are carried out (see Fig. 6*a*).

There is chemical evidence that the two interstitial carbon atoms, present in the parent carbonylate at the centres of the Ru_6 octahedra, are retained after the carbonyl groups are driven off thermally. This leaves the structure that is schematized in Fig. 6(*b*). Analysis of both Ru and Cu *K* XAFS results (of Fig. 6*b*) is broadly in agreement

(Shephard *et al.*, 1998) with this structure: there is certainly strong evidence for the existence of a 'base' of four copper atoms, each of which is attached *via* oxygen to a silicon atom of the underlying mesoporous silica.

XAFS alone, however, though much more revealing that XRD for this purpose, is not a powerful enough tool to permit us to determine the precise structure of the $Ru_{12}Cu_4C_2$ anchored cluster. It is necessary to invoke computational assistance.

In association with our colleagues Bromley and Catlow (Bromley *et al.*, 2000) we have employed a blend of interatomic-potential-based molecular-dynamics and energy-minimization simulations, which were used to obtain a range of approximate models of the cluster

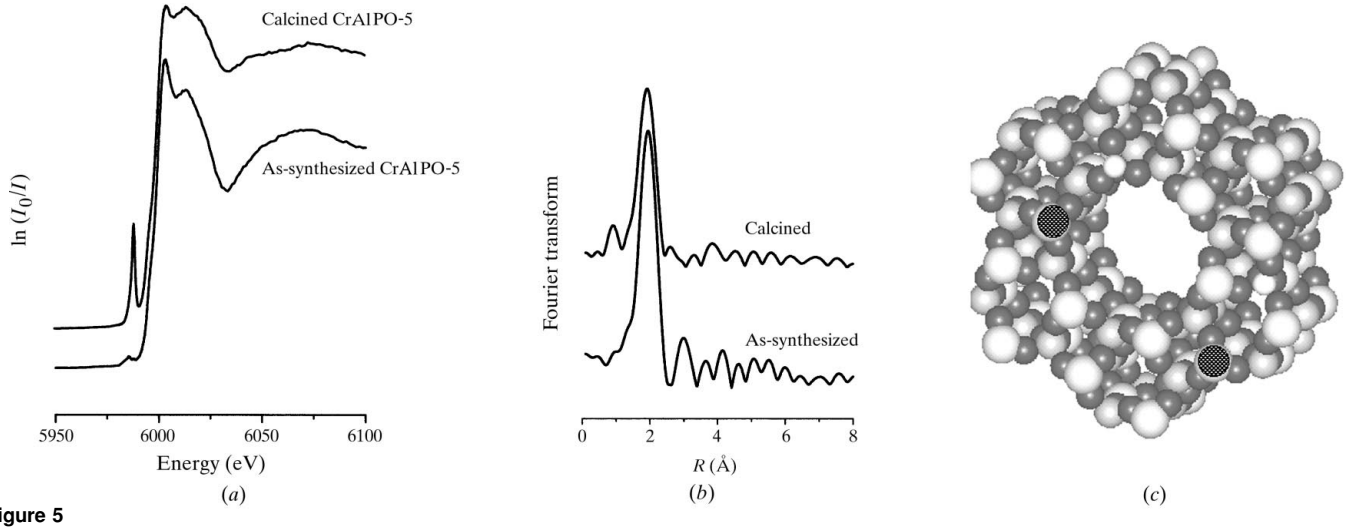

Figure 5
(*a*) Cr *K*-edge XANES and (*b*) Fourier transform magnitude of the microporous chromium-substituted aluminophosphate No. 5 (CrAlPO-5) catalyst used for selective oxidation of alkanes and cyclohexylhydroperoxide. (*c*) Computer graphic representation of the AlPO-5 structure. The as-prepared material contains chromium ions in the III state; when calcined in air to remove the occluded structure-directing organic templates (in this case tetraethylammonium hydroxide), part of the chromium ions are oxidized to oxidation state VI.

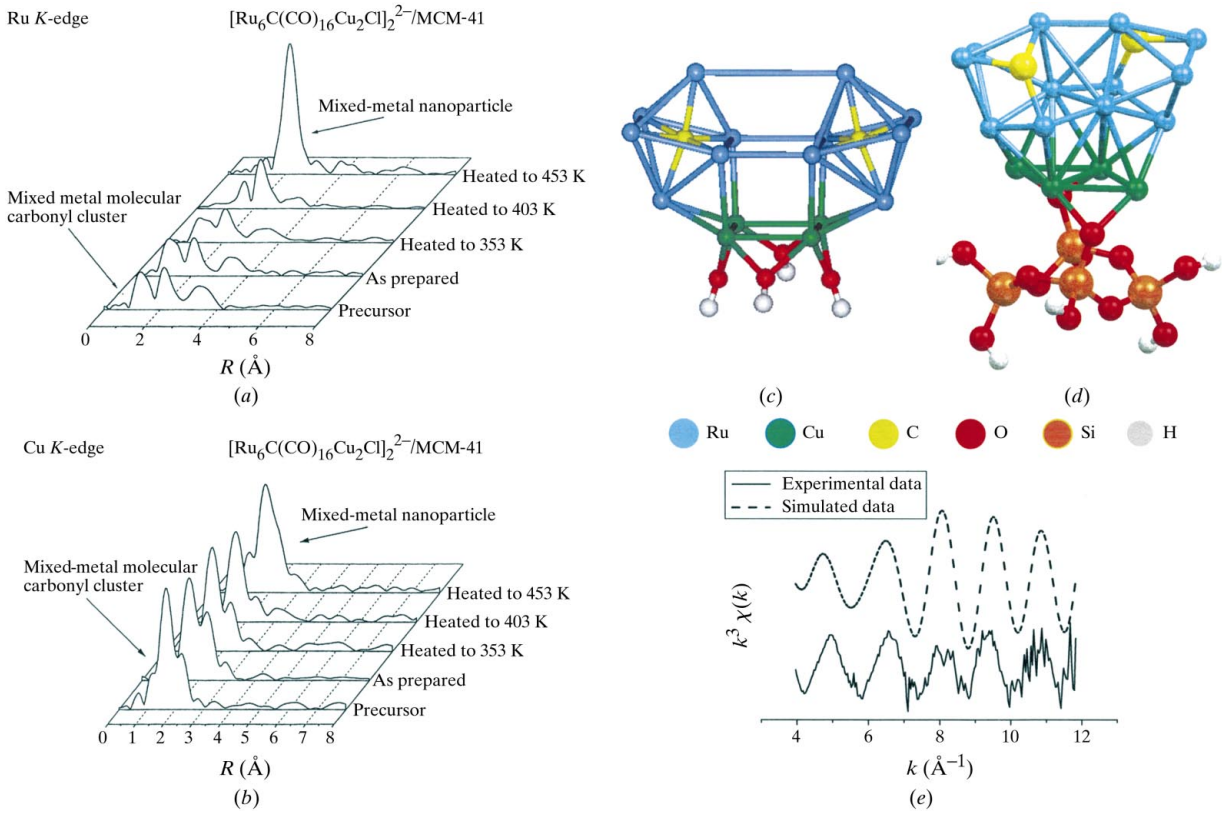

Figure 6
Fourier transform of the (*a*) Ru *K*-edge and (*b*) Cu *K*-edge EXAFS data recorded during the thermolysis of the $Ru_{12}Cu_4$/MCM-41 catalyst. (*c*) The model derived from a simple energy-minimization calculation. (*d*) The model based on a detailed DFT calculation. (*e*) Comparison of the Cu *K*-edge EXAFS data with the spectrum calculated taking the structural details obtained from the DFT calculation.

structures based upon the denuded parent carbonylate in free space. Preliminary molecular-mechanics simulations followed by single-point density functional theory (DFT) calculations were used to identify the lower energy free-space clusters. This procedure produced a number of cluster structures, all of which possessed the 'rosette' depicted in Fig. 6.

In further computations (Bromley *et al.*), the Cu–surface interaction was taken to be *via* Cu—O—Si, a fact established (see above) in our XAFS studies. [Such a link may be readily formed *via* a pendant silanol Si—O—H bond. It is noteworthy that, in a recent independent theoretical study (Lopez *et al.*, 1999) of minute Cu clusters bound to a silica surface, the Cu—O—Si link was found to be energetically favourable.] Using such linkages, the DFT-optimized rosette cluster was then 'grafted' onto various representations of the silica surface and geometry-optimized using DFT, using the program *Dmol*[3] (Delley, 1990, 1997). The results (one of which is shown in Fig. 6*d*) illustrate nicely the competing effects of bulk cluster relaxation and different support interations.

Here we see that there has been substantial movement of the carbon atoms from their original interstitial positions. A comparison of experimental and simulated XAFS results (Fig. 6*c*) is very encouraging.

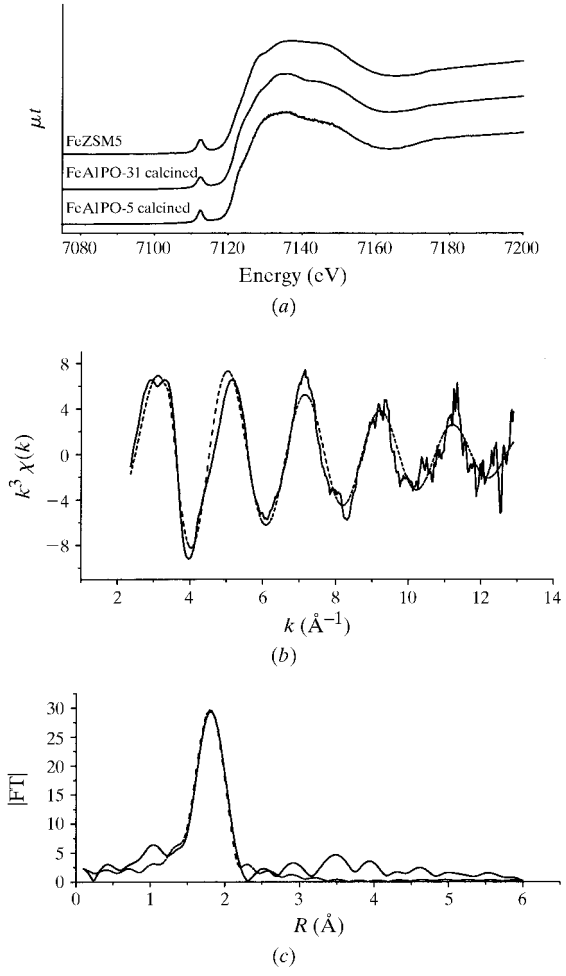

Figure 7
(*a*) Fe *K*-edge XANES data of the calcined FeAlPO-5, FeAlPO-31 and FeZSM-5 catalysts. (*b*) Fe *K*-edge EXAFS data of calcined FeAlPO-31. (*c*) Associated Fourier transforms. The solid line shows the experimental data and dashed curve represents the EXAFS calculated using the program *EXCURV*98.

At present there seem to be few, if any, other experimental tools that are sufficiently penetrating, first to arrive at the atomic architecture of the anchored cluster and, second, to locate precisely the positions taken up by the carbon atoms.

3.4. *Molecular-sieve catalysts for the regio- and shape-selective oxidation of alkanes*

Framework-substituted molecular-sieve aluminophosphate microporous solids are the 'centre pieces' of a new approach (Raja & Thomas, 1998; Thomas *et al.*, 1999*b*; Raja *et al.*, 2000) to the aerobic oxyfunctionalization of saturated hydrocarbons. The sieves and the few percent of the Al^{III} sites within them that are replaced by catalytically active transition-metal ions in high oxidation states (Co^{III}, Mn^{III}, Fe^{III}) are so-designed as to allow free access of oxygen into and out of the interior of these high-area solids. Certain metal-substituted molecular sieves permit only end-on approach of linear alkanes to the active centres, thereby favouring enhanced reactivity of terminal methyl groups. By optimizing the cage dimension with respect to that of the hydrocarbon reactant, as well as adjusting the average separation of active centres within a cage, and by choosing the sieve with the appropriate pore aperture, highly selective conversions can be achieved, such as 1-hexane to hexanoic acid and a few C_2 products,

$$\begin{array}{c} CH_3(CH_2)_4CH_3 \\ O_2 \downarrow 4\%\ Co-\ or \\ Mn-substituted\ AlPO-18 \\ CH_3(CH_2)_4CO_2H + CH_3CH(OH)(CH_2)_3CH_3 + CH_3C(O)(CH_2)_3CH_3 \end{array} \quad (2)$$

or 1-hexane to adipic acid,

$$\begin{array}{c} CH_3(CH_2)_4CH_3 \\ O_2 \downarrow 10\%\ Co-substituted\ AlPO-18\ or\ AlPO-34 \\ CO_2H(CH_2)_4CO_2H \end{array} \quad (3)$$

Moreover, with the right choice of molecular sieve and metal-ion active centre, cyclohexane may be selectively converted to cyclohexanol, cyclohexanone and adipic acid. The great merit of the Co^{III} (Mn^{III}) AlPO catalysts is that such reactions may be effected at low temperature and heterogeneously using air as oxidant (Kellog, 2000). Adipic acid [the product of reaction (3) above] is also produced in high yield when cyclohexane is aerobically oxidized over a so-called Fe^{III}AlPO-31 catalyst. We have described elsewhere (Dugal *et al.*, 2000, Fig. 14 therein) how XAFS analysis pinned down the nature of the active site in this catalyst. The XAFS-derived Fe—O coordination number, bond distance and Debye–Waller factor are, respectively, 3.85 ± 0.40, 1.85 (2) Å and 0.0045 $Å^2$ (see Fig. 7).

When Co (Mn) AlPO catalysts are used for selective oxidation reactions, determinations of the nature of the active site, under controlled atmosphere, are more convenient to record than under reaction conditions (because of safety considerations arising from relatively high-pressure operation of the catalytic reactor). With solid acid catalysts (Chen & Thomas, 1994; Thomas *et al.*, 1994) (such as Co^{II}AlPO-18), however, because reactions such as the dehydration of methanol to light olefins proceed smoothly at atmospheric pressure, *in situ* determination of the nature of the Co^{II}-centred site (with its loosely attached proton bound to a nearby framework oxygen functioning as a Brønsted acid) may be readily carried out.

4. Concluding comments

XAFS has already proved invaluable in our and other workers hands (Clausen *et al.*, 1998; Bando *et al.*, 1996; Chun *et al.*, 1996; Ohata, 1998; Koningsberger & Mojet, 2000; Knop-Gericke *et al.*, 2000; Edelmann *et al.*, 2000; Pillep *et al.*, 1999), ever since it first (Kozolowski *et al.*, 1983) began to be used to probe the structures of model catalytic systems (under rather poorly defined ambient conditions). Now that it has become almost routine to establish the electronic and atomic structure of catalytically active solids (which constitute no more than a percent of all the atoms present) on time scales of fractions of a second and upwards, we now await progress that will take the time domain of measurement to the nanosecond or beyond. Ideally, just as in the new realm of femtochemistry opened up by Zewail (2000), one would wish to be able to harness new developments in synchrotron physics, of the type described at XAFS XI by David Norman (2001), so as to permit perhaps nano- or picosecond resolution in acquiring XAFS data. By achieving this target, the dynamics of bond breaking and bond making, and consequential atomic rearrangement, will become accessible.

JMT acknowledges continued support from EPSRC (UK) and GS thanks the Leverhulme trust for a Senior Research Fellowship

References

Aletru, C., Greaves, G. N., Sankar, G. & Kempsen, V. (1999). *Jpn J. Appl. Phys.* **38**, 97–100.

Als-Nielsen, J., Grubel, G. & Clausen, B. S. (1995). *Nucl. Instrum. Methods B*, **97**, 522–525.

Bando, K. K., Asakura, K., Iwasawa, Y., Arokawa, H. & Elsobe, K. (1996). *J. Phys. Chem.* **100**, 13636–13645.

Bromley, S. T., Sankar, G., Catlow, C. R. A. & Thomas, J. M. (2000). *Microporous Mesoporous Mater.* In the press.

Chen, J. & Thomas, J. M. (1994). *J. Chem. Soc. Chem. Commun.* pp. 603–604.

Chun, W.-J., Asakura, K. & Iwasawa, Y. (1996). *Appl. Surf. Sci.* **101**, 143–146.

Clausen, B. S. & Topsøe, H. (1996). *X-ray Absorption Fine Structure for Catalysts and Surfaces*, edited by Y. Iwasawa, ch. 7.5. Singapore: World Scientific.

Clausen, B.-S., Topsøe, H. & Frahm, R. (1998). *Adv. Catal.* **42**, 315–344.

Couves, J. W., Thomas, J. M., Waller, D., Jones, R. H., Dent, A. J., Derbyshire, G. E. & Greaves, G. N. (1991). *Nature (London)*, **354**, 465–468.

Delley, B. (1990). *J. Chem. Phys.* **92**, 508–517.

Delley, B. (1997). *Dmol*^{3} *User Guide*, MSI, San Diego, USA.

Dugal, M., Sankar, G., Raja, R. & Thomas, J. M. (2000). *Angew. Chem.* **39**, 2310–2313.

Edelmann, A., Scheisser, W., Vinek, H. & Jentys, A. (2000). *Catal. Lett.* **69**, 11–16.

Ertl, G., Knozinger, H. & Weitkamp, J. (1997). *Handbook of Heterogeneous Catalysis*. Weinheim: Wiley VCH.

Gleeson, D., Sankar, G., Catlow, C. R. A., Thomas, J. M., Spano, G., Bordiga, S., Lamberti, C. & Zecchina, A. (2000). *Phys. Chem. Chem. Phys.* **2**, 4812–4817.

Kellogg, R. M. (2000). *Chemtracts*, **13**, 33–37.

Knop-Gericke, A., Havecker, M., Schedel-Niedrig, Th. & Schlogl, R. (2000). *Top. Catal.* **10**, 187–198.

Koningsberger, D. C. & Mojet, B. (2000). Editors. *Role and Contribution of XAFS Spectroscopy in Catalysis*, *Top. Catal.* **10**, special issue.

Kozlowski, R., Pettifer, R. F. & Thomas, J. M. (1983). *J. Phys. Chem.* **87**, 5172–5176.

Lopez, N., Illas, F. & Pachioni, G. (1999). *J. Phys. Chem. B*, **103**, 1712–1718.

Maschmeyer, T., Rey, F., Sankar, G. & Thomas, J. M. (1995). *Nature (London)*, **378**, 159–162.

Murugavel, R. & Roesky, H. W. (1997). *Angew. Chem.* **36**, 477–479.

Nishimura, M. (1993). PhD thesis, University of London (Royal Institution).

Nishimura, M., Sankar, G. & Thomas, J. M. (2001). In preparation.

Norman, D. (2001). *J. Synchrotron Rad.* **8**, 72–75.

Ohata, T. (1998). *J. Electron Spectrosc.* **92**, 131–139.

Oldroyd, R. D., Sankar, G. & Thomas, J. M. (1997). *Chem. Commun.* pp. 2025–2026.

Oldroyd, R. D., Sankar, G., Thomas, J. M., Hunnius, M. & Maier, W. F. (1998). *J. Chem. Soc. Faraday Trans.* **94**, 3177–3182.

Pillep, B., Behrens, P., Schubert, U.-A., Spengler, J. & Knozinger, H. (1999). *J. Phys. Chem.* **103**, 9595–9603.

Raja, R., Sankar, G., Hermans, S., Shephard, D. S., Bromley, S., Thomas, J. M., Johnson, B. F. G. & Maschmeyer, T. (1999). *Chem. Commun.* pp. 1571–1572.

Raja, R., Sankar, G. & Thomas, J. M. (2000). *Angew. Chem.* **39**, 2313–2316.

Raja, R. & Thomas, J. M. (1998). *Chem. Commun.* pp. 829–830.

Rey, F., Sankar, G., Maschmeyer, T., Thomas, J. M., Bell, R. G. & Greaves, G. N. (1996). *Top. Catal.* **3**, 121–134.

Roberts, M. A., Sankar, G., Thomas, J. M., Jones, R. H., Du, H., Chen, J., Pang, W. & Xu, R. (1996). *Nature (London)*, **381**, 401–404.

Sankar, G. & Thomas, J. M. (1999). *Top. Catal.* **8**, 1–21.

Sankar, G., Thomas, J. M. & Catlow, C. R. A. (2000). *Top. Catal.* **10**, 255–264.

Sankar, G., Wright, P. A., Natarajan, S., Thomas, J. M., Greaves, G. N., Dent, A. J., Dobson, B. R., Ramsdale, C. A. & Jones, R. H. (1993). *J. Phys. Chem.* **97**, 9550–9554.

Sheldon, R. A. (1983). *J. Mol. Catal.* **20**, 1.

Shephard, D. S., Maschmeyer, T., Sankar, G., Thomas, J. M., Ozkaya, D., Johnson, B. F. G., Raja, R., Oldroyd, R. D. & Bell, R. G. (1998). *Chem. Eur. J.* **4**, 1214–1224.

Thomas, J. M. (1997). *Chem. Eur. J.* **3**, 1557–1562.

Thomas, J. M. (1999). *Angew. Chem Int. Ed. Engl.* **38**, 3589–3628.

Thomas, J. M. & Greaves, G. N. (1994). *Science*, **265**, 1675–1676.

Thomas, J. M., Greaves, G. N. & Catlow, C. R. A. (1995). *Nucl. Instrum. Methods B*, **97**, 1–10.

Thomas, J. M., Greaves, G. N., Sankar, G., Wright, P. A., Chen, J., Dent, A. J. & Marchese, L. (1994). *Angew. Chem. Int. Ed. Engl.* **33**, 1871–1873.

Thomas, J. M., Raja, R., Sankar, G. & Bell, R. G. (1999). *Nature (London)*, **398**, 227–230.

Thomas, J. M., Sankar, G., Klunduk, M. C., Attfield, M. P., Maschmeyer, T., Johnson, B. F. G. & Bell, R. G. (1999). *J. Phys. Chem.* **103**, 8809–8813.

Thomas, J. M. & Thomas, W. J. (1997). *Heterogeneous Catalysis: Principles and Practice*. Weinheim: Wiley VCH.

Zewail, A. H. (2000). *Angew. Chem. Int. Ed.* **39**, 2586–2631.